

FacAID: A Transformer Model for Neuro-Symbolic Facade Reconstruction

ALEKSANDER PŁOCHARSKI, Warsaw University of Technology, Poland and IDEAS NCBR, Poland

JAN SWIDZINSKI, IDEAS NCBR, Poland

JOANNA PORTER-SOBIERAJ, Warsaw University of Technology, Poland

PRZEMYSŁAW MUSIALSKI, New Jersey Institute of Technology, USA and IDEAS NCBR, Poland



Fig. 1. A rendering of a street scene with procedural facades all generated by our method. Novel scene variations can be crafted in the matter of minutes.

We introduce a neuro-symbolic transformer-based model that converts flat, segmented facade structures into procedural definitions using a custom-designed split grammar. To facilitate this, we first develop a semi-complex split grammar tailored for architectural facades and then generate a dataset comprising of facades alongside their corresponding procedural representations. This dataset is used to train our transformer model to convert segmented, flat facades into the procedural language of our grammar. During inference, the model applies this learned transformation to new facade segmentations, providing a procedural representation that users can adjust to generate varied facade designs. This method not only automates the conversion of static facade images into dynamic, editable procedural formats but also enhances the design flexibility, allowing for easy modifications and variations by architects and designers. Our approach sets a new standard in facade design by combining the precision of procedural generation with the adaptability of neuro-symbolic learning.

CCS Concepts: • **Computing methodologies** → **Shape modeling; Neural networks**.

Additional Key Words and Phrases: neurosymbolic, procedural generation, facade modeling, transformers

1 INTRODUCTION

The field of architectural modeling in computer graphics has greatly advanced with the adoption of procedural methods, enabling the efficient generation of vast and complex urban structures and environments [Müller et al. 2006; Wonka et al. 2003]. However, the creation of grammar rules and their parameters is time-consuming and requires specific knowledge and skills, posing a barrier for non-experts. In response, researchers in computer graphics introduced

inverse procedural modeling to extract procedural rules from existing models or images, simplifying the process and making it more accessible [Musialski and Wimmer 2013; St’ava et al. 2010; Wu et al. 2014].

Inverse methods, however, came with new problems, like their complexity, error-proneness, and limited variability and flexibility. To address this, our work introduces a novel neuro-symbolic [Ritchie et al. 2023] approach to enhance facade design. This integration combines neural networks’ learning capabilities with procedural models’ symbolic reasoning, creating a robust framework for complex architectural modeling. We propose a transformer-based model that converts flat, segmented facade structures into hierarchical procedural definitions using a custom-designed shape grammar [Stiny 1975] tailored for architectural facades [Wonka et al. 2003].

Our model is trained on a dataset of segmented facade structures and their corresponding procedural definitions, aiding the model in understanding and replicating structural nuances while aligning with architectural principles. During inference, the model applies learned transformations to new segmented images, converting them into procedural formats. This allows users to generate variations of designs, adjust elements, or create new facades within an established procedural framework, enhancing design flexibility and creativity. Figure 1 shows a urban scene designed by a digital artist using facades generated with our system.

The key contributions of our work include: (1) A neuro-symbolic transformer-based model that automates the conversion of segmented facades into editable procedural definitions. (2) A custom-designed split grammar specifically for architectural facades. (3) A novel dataset of facade structure and their procedural definitions, serving as a training and validation foundation. (4) Demonstrations of the model’s practical application in generating varied facade designs, showcasing its utility.

Authors’ addresses: Aleksander Płocharski, Warsaw University of Technology, Poland and IDEAS NCBR, Poland; Jan Swidzinski, IDEAS NCBR, Poland; Joanna Porter-Sobieraj, Warsaw University of Technology, Poland; Przemyslaw Musialski, New Jersey Institute of Technology, USA and IDEAS NCBR, Poland.

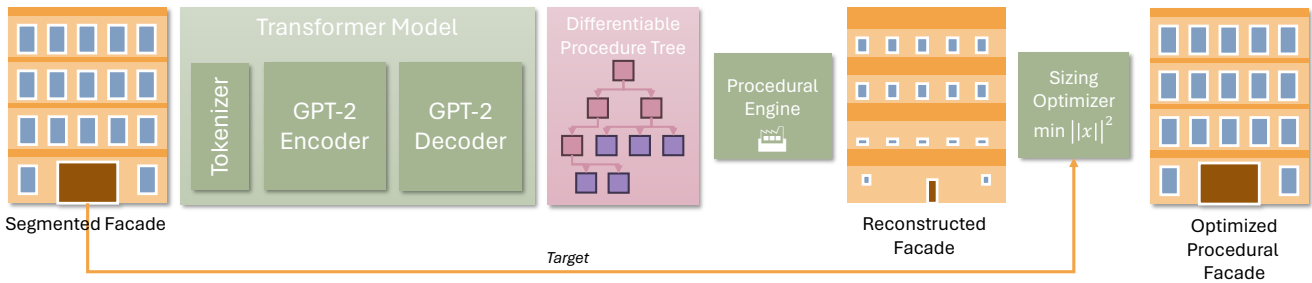


Fig. 2. The inference and modeling pipeline of our method: (1) we start with a user provided segmented facade; (2) after preprocessing, a transformer-based model inversely extracts the procedure how to generate the facade; (3) it can be regenerated procedurally, or used for interactive generation of new variations or other facades.

2 RELATED WORK

Procedural Modeling. Our work builds on grammar-based procedural methods, introduced for modeling of geometry in botany [Prusinkiewicz and Lindenmayer 1990] and design [Stiny 1975]. For modeling of architecture, shape grammars [Stiny 1975] based on splitting rules turned out to be well suitable [Müller et al. 2006; Whiting et al. 2009; Wonka et al. 2003]. Such rules decompose geometric shapes into hierarchical structures, making it easier to manage and manipulate complex designs. The primary objective of our work is to automatically infer proper production rules from a grammar given an input segmented facade, which allows for user-friendly editing and generation of new variations [Bao et al. 2013; Ilčík et al. 2015; Lipp et al. 2008].

Inverse Procedural Modeling. Inverse procedural modeling aims to derive shape grammars from given segmented geometry or imagery. Early work introduced grammars that split building but each rule was crafted and applied manually [Aliaga et al. 2007; Bekins and Aliaga 2005]. Subsequent research has continued along this path, proposing various methods to extract procedural descriptions from facades [Becker 2009; Demir and Aliaga 2018; Müller et al. 2007; Teboul et al. 2011, 2013]. Notably, the work on inverse procedural modeling of vector-art provided a formal treatment of the problem in graphics [St’ava et al. 2010].

A significant challenge in inverse procedural modeling is dealing with noisy or unsegmented inputs, where lower-level shape understanding and symmetry detection become crucial [Bokeloh et al. 2010; Müller et al. 2007]. Once shape grammars are learned from typical input facades, they can be used as priors to guide further reconstruction efforts, a line of work explored by several research groups [Mathias et al. 2011; Riemenschneider et al. 2012; Ripperda and Brenner 2009; Teboul et al. 2013; Toshev et al. 2010; Vanegas et al. 2010].

There have been multiple approaches to extract grammars from simple facades [Weissenberg et al. 2013], also with varying alternative subdivision rules [Zhang et al. 2013]. Additionally, the concept of Bayesian models merging to combine deterministic grammars into a stochastic one has been explored, but it necessitates a robust initial grammar [Martinovic and Gool 2013; Talton et al. 2012], or a predefined grid-layout structures [Fan et al. 2014]. Learning of grammars based on the smallest-grammar paradigm [Charikar et al. 2005] using approximate dynamic programming [Wu et al. 2013]

has also been proposed. In contrast, our approach does rely on predefined rules based on a split grammar [Wonka et al. 2003], but it uses neuro-symbolic transformer model to convert all segmented facade images into procedural representations robustly, streamlining the process of rule applications.

Generative Models in Graphics. Generative models have advanced significantly in recent years, particularly in modeling 2D images [Karras et al. 2018] and 3D shapes [Nash et al. 2020]. These models often use latent space projections to generate new data [Richardson et al. 2020]. In the context of building facade images, generative models create realistic urban images, which, although detailed, are often limited in resolution and lack high-level structure or parameterization [Bachl and Ferreira 2019; Sun et al. 2022]. Our work addresses these shortcomings by focusing on generating procedural graphs, allowing for enhanced flexibility and customization in facade design.

Neuro-Symbolic Methods in Graphics. Program synthesis, a concept dating back to 1957 [Backus et al. 1957], explores methods for automatically generating programs from high-level specifications. Inductive synthesis, which relies on partial user specifications and search methods, has seen significant advances in specifying user intent through input-output examples, demonstrations, and natural languages [Alur et al. 2013; Solar-Lezama et al. 2006].

In computer graphics, these methods combine the strengths of generative AI and symbolic programs to represent, generate, and manipulate visual and geometric content [Ritchie et al. 2023]. Graph-based models for procedural content generation have been extensively studied, with recursive neural networks capturing dependencies like adjacency and symmetry within shapes [Li et al. 2017; Mo et al. 2019]. These models have evolved to generate shape programs using recurrent networks and transformers [Jones et al. 2020; Nash et al. 2020]. In CAD modeling, deep learning has enabled the creation of complex designs from textual descriptions, exemplified by models like DeepCAD [Wu et al. 2021], and generative models that produce diverse, high-quality procedural materials [Guerrero et al. 2022]. Our approach also uses an autoregressive transformer model to convert segmented facade structures into procedural definitions.

Program synthesis transforms modeling into code generation, as seen in reverse-engineering CAD programs from 3D shapes [Du et al. 2018; Nandi et al. 2018] and shape program manipulation [Hempel et al. 2019]. Recent work in program rewrites generates compact 3D

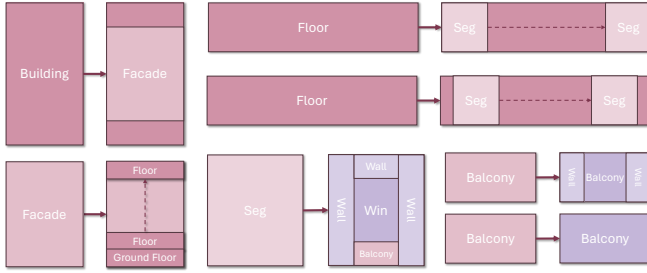


Fig. 3. Example production rules of our split grammar which follows the notion as proposed by Wonka et al. [2003]. The depicted productions are a subset of all productions P . For a full set of rules used by our grammar please refer to supplemental material.

CAD code using E-graphs, optimizing design and fabrication plans [Nandi et al. 2019]. Neuro-symbolic programming combines neural networks with symbolic reasoning to enhance model interpretability and flexibility, applicable across various domains [Chaudhuri et al. 2021; Li et al. 2023].

By integrating neuro-symbolic learning with a custom-designed split grammar, our model automates the conversion of segmented facade structures into procedural definitions, providing a dynamic tool for architects and designers to create and modify facade layouts.

3 PROBLEM STATEMENT AND OVERVIEW

The main idea of our method is to enable a transformer-based network to infer procedural descriptions from annotated flat grid-like segmentations. The grammar of the procedures is based on split-grammars as proposed by Wonka et al. [2003] and subsequent work. The control of the grammar is encoded in a heuristic module which we design based on typical architectural rules [Wonka et al. 2003].

The main assumption is that an “oracle” data generator, composed of a grammar and heuristics, constitutes the rules. All our data is generated by that generator using stochastic seeding. The resulting procedures are expanded down to the terminal level, which becomes the input to the transformer. In other words, the generator is considered a “black box,” whose inverse operation the transformer attempts to learn. Thanks to this approach, in contrast to other inverse procedural methods [Wu et al. 2013], we aim for the procedures to function in a unified space of programs defined by the “black box,” rather than requiring the careful construction of a specialized single-use language for each given facade.

The whole system is composed of three main modules (cf. Fig. 2):

- (1) A transformer neural model for neuro-symbolic learning,
- (2) a procedural engine, and
- (3) an optimization module for sizing adjustments.

During the inference, segmented facade abstractions are passed as input to the transformer model. It then predicts a procedure that correlates with the underlying structure of the input facade. After this step, a hierarchical procedural representation of all the facade elements is generated, but the sizing parameters are not yet set at this stage. As the created procedure is differentiable wrt the sizing parameters, a second module—the optimizer—minimizes the MSE between the target and the procedural result on pixel level basis.

4 PROCEDURAL DATA GENERATION

To our best knowledge, there are no publicly available datasets that contain facades annotated with their procedural definitions of any kind. To create a dataset with facades and their procedural definitions, we developed a split grammar system, drawing on facade modeling techniques from previous work [Wonka et al. 2003]. Our grammar includes around 30 production rules that range from simple symbol replacements to complex pattern formations and involves 16 terminal and 12 non-terminal symbols. Please refer to Figure 3 and supplemental material for visual depiction.

A random derivation of the grammar’s rule-set will still generate a non-plausible facade in the vast majority of cases. To address this, we implemented a generator that is able to generate a varied distribution of coherent facades based on architectural rules and heuristics. The generation process begins with a selection from style-specific subsets of arguments to maintain consistency. We define the chosen style-specific subset as S . The generator is initialized with a starting non-terminal n_0 and employs a heuristic module $H_p(S)$ to pick the next production to apply while maintaining architectural suitability. Another module, $H_a(S)$, adjusts the arguments of the selected production rule for structural soundness and coherence with the rest of the facade. This sequence of applying rules and adjusting arguments continues until all non-terminals are transformed into terminals, leaving a complete facade and a derivation tree that documents the creation process, and which can be executed in order to regenerate the facade.

It is those trees of productions that form the language of the procedures we focus on generating. Because of the nature of their structure, they are similar to other node-based procedural systems like shader graphs, but instead of performing mathematical calculations, each node partitions the space provided as the input to the node.

5 NEURO-SYMBOLIC GENERATIVE MODEL

In this section we describe our core contribution, the transformer-based model for neuro-symbolic generation of procedures from flat facade segmentation.

5.1 Transformer-Based Inverse Procedural Learning

Our model is inspired by recent works which utilize transformers [Vaswani et al. 2017] to represent and generate geometric entities, like plants [Lee et al. 2024], floor-plan layouts [Para et al. 2021] or apartment layouts [Leimer et al. 2022; Paschalidou et al. 2021; Wang et al. 2020]. In contrast to the decoder-type models of previous work, our model is comprised of a transformer-based encoder g_θ which then provides its outputs as context for a transformer-based sequence generator/decoder h_ϕ . We implement g_θ and h_ϕ as GPT-2 models [Radford et al. 2019] using the implementation included in the Hugging Face library [Wolf et al. 2020].

Sequence Generation: A transformer-based encoder g_θ takes a sequence S and generates a sequence aware embedding e_i for each sequence element s_i . Together the embeddings create a new sequence $g_\theta(S) = E$ that encodes the information contained in S . A transformer-based sequence generator h_ϕ factors the probability distribution over sequences S into a product of conditional probabilities

over individual tokens:

$$p(S | \phi) = \prod_i p(s_i | s_{<i}, \phi),$$

where $s_{<i} := s_1, \dots, s_{i-1}$ denotes the partial sequence up to the token s_{i-1} . Given a partial sequence $s_{<i}$, a sequence generator h_ϕ predicts the probability distribution over all possible discrete values of the next token: $h_\phi(s_{<i}) = p(s_i | s_{<i}, \phi)$. The distribution can then be sampled to acquire the value of s_i .

Our model additionally conditions the sequence generator h_ϕ using the output from the encoder using the cross-attention mechanism extending it to $h_\phi(E, s_{<i}) = p(s_i | E, s_{<i}, \phi)$ where E is the encoding of the input sequence. The whole model can then be defined as

$$f_{\theta, \phi}(S_I, s_{<i}) = h_\phi(g_\theta(S_I), s_{<i})$$

where S_I is the input sequence and $s_{<i}$ are the values from the output sequence that have already been generated.

Tokenization: In order to feed the data through our model, the inputs and outputs need to be converted into sequences of tokens, respectively S_I and S_O . The input sequence represents a facade segmentation comprised of non-overlapping rectangles of different classes. Each rectangle r_i is represented by 5 tokens $(t_i, o_i^x, o_i^y, w_i, h_i)$ where t_i indicates the grammar terminal symbol which the rectangle represents, o_i^x and o_i^y are the coordinates of its bottom-left corner and w_i and h_i are respectively its width and height. All of the rectangles r_i are then sorted based on the position of their bottom-left corners (first by the Y coordinate then X), in order to decrease the variability of the input sequences that represent the same facades, and concatenated to form the sequence S_I . Formulating the output procedures as sequences S_O poses a greater challenge. Since the procedures take the form of rooted trees we employ the breadth-first traversal method (starting from the root) to produce a sequence of nodes n_i . After that we can resume with a similar approach as with the inputs - each node n_i is represented by its class c_i and the set of its structural parameters (p_i^1, \dots, p_i^j) which can be either integer or floating point values. The nodes n_i are then concatenated with separator tokens in-between them. When undergoing the tokenization process both categorical and integer parameters are translated exactly into their token counterparts whereas continuous values, like positions and sizes, are discretized between their edge values with a given resolution. After that the model can be trained on all the generated input-output sequence pairs of facade segmentations and their procedural representations.

Positional Encodings: We employ the usual transformer approach and feed the model with not only the sequences of tokens but also the information about their positions in the sequence. Each token is tagged with its global position in either the input or output sequence. Additionally, since our rectangle sequences are represented by groups of 5 tokens we assign each of them a local index from 0 to 4 signifying their location in the sequence of 5 [Leimer et al. 2022]. We extend this approach to the output sequences and assign the output tokens a local index in groups that encompass a single production and its arguments. In this case the groups are of dynamic length.

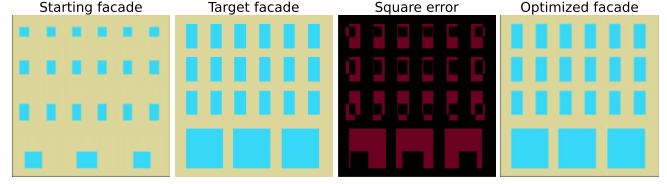


Fig. 4. Sizing optimizer: The input to sizing optimization is the reconstructed procedure (structural) with default sizing information. As our derived procedures are differentiable wrt the sizing parameters, the terminal sizes are computed by optimizing the square error.

Training: The tokenized sequence pairs and their positional encodings are then fed through our model in batches. After each batch we perform an optimization step using the AdamW optimizer [Loshchilov and Hutter 2019]. This process of going through the whole dataset in batches repeats until the loss function reaches a local minimum or the model starts overfitting to the training data.

5.2 Neuro-Symbolic Procedure Inference

The neuro-symbolic generation (inference) is performed by providing a segmented facade image, which can be done using interactive methods [Musiański et al. 2012] or by using automatic facade segmentation [Tyleček and Šára 2013] or building labeling methods [Selvaraju et al. 2021]. In the following we consider the input facade segmentation is given and represented as a flat irregular 2D grid of boxes with their classes (e.g., *Window*, *Balcony*, etc.) and extents.

The segmentation is then tokenized using the approach described in Section 5.1. It is crucial that the same tokenization scheme is used here as was used for the training data for the model. The encoding of the input sequence $g_\theta(S_I)$ is calculated and the generation of the output sequence, conditioned on this encoding, begins. The inference is performed one token at a time to make sure the resulting procedure will be syntactically valid and executable. To achieve that at each step of the generation process we perform invalid state nullification—we manually set generated probabilities $p(s_i | E, s_{<i}, \phi)$ for syntactically invalid choices to zero and re-normalize the probability distribution. The impact of this step can be seen in Table 1 which showcases how the average negative log likelihood loss changes after applying this modification for models trained on different amounts of data. The token generation process repeats until an end of sequence token is generated.

The result of the inference is a brand new procedure that regenerates the structure of the flat rectangle representation when executed. Subsequently, the user is free to adjust the parameters of the procedure and create new facade variations.

5.3 Differentiable Procedure Sizing Optimization

The model inference process leaves us with a structurally sound representation of the input facade but all of its sizing parameters are set to default values. In order to fully reproduce the input facade the procedure needs to go through the optimization module which finds the proper values of the sizing parameters. This module heavily leverages the fact that we have implemented all of our production

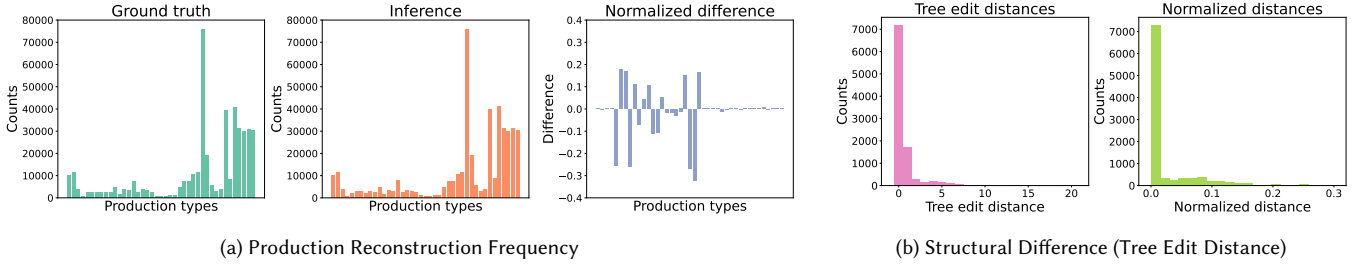


Fig. 5. Quantitative evaluation of our model: The first metric shows the frequency of the usages of the procedural rules between the ground truth and reconstructions as well as their difference normalized by inference counts. The second metric measures how much tree-edits are needed to change the reconstructed rules to those from ground truth. The normalized distances represents edit distances divided by their original tree size.

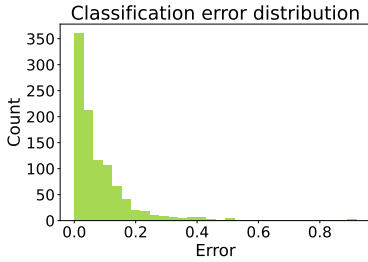


Fig. 6. Optimized facades classification error distribution: Showcases how closely the optimized result of our pipeline matches with the input segmentation. The error measures what percentage of the resulting segmentation does not perfectly overlap the input.

rules in a way that makes them differentiable with respect to their sizing parameters. This means that when the procedure is executed all positions and sizes of resulting rectangles can be expressed as differentiable functions of the parameters of the procedure. We use this property to perform a gradient based optimization.

In order to perform the optimization we define a loss function that enables the model to sequentially approach the input facade segmentation. We treat the input segmentation as an image and then calculate the mean square error between it and the result of executing our procedure (Figure 4). The engine result also needs to be rasterized since it’s a a sequence of rectangles. To keep the function differentiable we rasterize all of the rectangles in a soft manner—using a combination of sigmoid functions positioned at the edges of the rectangles. This allows us to calculate the gradient of the mean square error with respect to all of the sizing parameters of the procedure.

Table 1. The average negative log likelihood loss of our model based on a test set of 10k facades. Both rows show the test loss obtained using models trained on different amounts of data (50k, 100k and 200k facades respectively) with and without Invalid State Nullification (refer to Section 5.2).

	50k	100k	200k
without nullification	0.61404	0.34671	0.21412
with nullification	0.06301	0.04868	0.02519

We use the Adam optimizer [Kingma and Ba 2017] to iteratively minimize the loss and optimize the sizing parameters. The process ends once the loss function reaches a local minimum. After that we are left with a procedure that when executed matches the input flat rectangle representation exactly, while also further allowing the user to generate similar variations of the design.

5.4 Implementation and Training

We have implemented our system using Python and the PyTorch library. We trained our model using datasets of varying sizes (50k, 100k, 200k) on a NVIDIA L4 24GB and NVIDIA A100 40GB graphics cards. The training time for 50k samples was 13h on the L4, and 2.8 times faster on the A100 (5h, 10h, 20h respectively for each training data size). For most of our subsequent quantitative results we used the 50k dataset, as it has the same convergence behavior as the bigger sets (cf. Fig 7a), however, the qualitative results presented below were generated using the 200k samples dataset.

6 QUANTITATIVE EVALUATION

In this section we evaluate the performance of the model’s reconstruction abilities of the ground truth grammar. It is a key evaluation which shows that a transformer model can reconstruct a semi-complex split grammar, as proposed in Section 4.

6.1 Procedure Reconstruction Frequency

To perform the structural evaluation we have reconstructed 10k facade structures from a test data set, never before seen by our model, generated using the data generator described in Section 4. In Figure 5a we present the usage frequency of productions of our split-grammar in the 10k facades dataset. First, from the ground truth derivation trees and second, from the trees generated by our model. We observe that the model is able to closely approximate the behavior and heuristics of the data generator. The differences highlighted on the third plot mostly arise from the model alternating between productions that have similar visual effect which suggests its generalization abilities when reconstructing geometrical structures.

6.2 Procedure Structural Difference: Tree Edit Distance

The structural reconstructions are also measured against the ground truth based on the number of edits required in order to arrive at a

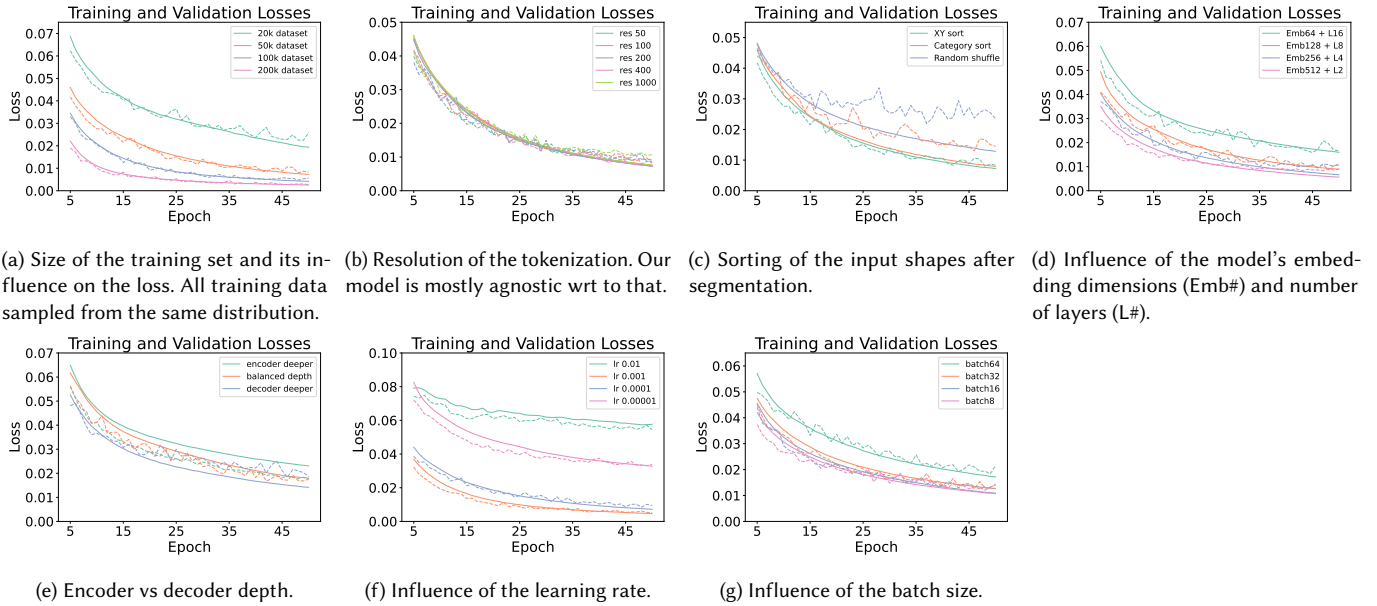


Fig. 7. Ablations of our model during training and validation measured using the teacher forcing cross-entropy loss. The solid curves show the training loss and the dashed curves show the validation loss. For a more detailed discussion of the ablation refer to Section 7. Please note, plots start at epoch 5.

precise reconstruction of the ground truth derivation tree. We use tree edit distance as our metric of the edits assuming that a single edit can amount to the following changes in the tree: (1) removing a node, (2) adding a node, (3) relabeling a node (changing its production type). Figure 5b shows that the majority of our structural reconstructions does not require any edits, while a vast majority requires no more than 5 editing steps. This, in most cases, means that less than 10% of the total tree needs to be modified to arrive at the ground truth structure.

6.3 Reconstruction Classification Error

We perform the quantitative measure of the optimized module on 1k, of the generated 10k, facade structures. The structures are optimized against a target segmentation from the ground truth. The metric used to compare the result with the input facade calculated what percentage of the segmentation does not match the ground truth exactly. In most cases the optimizer is able to adjust the parameters of the structural representations almost exactly, while a vast majority of the facades has an at least 80% match with the ground truth (cf. Fig. 6).

7 MODEL ABLATIONS

In this section we evaluate the performance of our model depending on various ablations of the setup; the charts are depicted in Fig. 7.

Tokenization Resolution. We have trained our model on 5 different segmentation discretization resolutions. Starting from a fine grid—1000x1000, all the way to a very coarse one—50x50. The results (cf Figure 7b) show that the resolution has little to no impact on the model’s ability to learn. We assume that this might be caused by the fact that the model learns the structure mostly based on the order

and counts of the rectangles that form the input segmentation and their geometric parameters (positions and sizes) just offer additional guidance in which case even the coarse discretization grid should be sufficient. After all, for a single facade structure, there exist multiple sizing variations.

Encoder Depth vs Decoder Depth. Since the model is composed of two distinct elements—encoder and decoder—we have tested whether making one of them bigger than the other would be beneficial to the learning process. We observe that the model with a deeper decoder tends to overfit a bit faster while making the encoder deeper produces the opposite result (cf Figure 7e). That is why we opt for a balanced architecture, as the validation curve of such a model correlates most closely with its training counterpart.

Embedding Dimensions vs Number of Layers. The model was also tested against its overall width and depth. We have varied those parameters by a factor of 2 for each of them. The results show that the model performs best when the number of its embedding dimensions (width) greatly surpasses its number of layers (cf Figure 7d). We conclude that this result most likely comes from the fact that the transformer model architecture already provides a lot of depth in its structure by feeding the embeddings through the quite shallow blocks multiple times. This allows the embeddings to pick up additional context information while their larger size provides the space required to store more of the nuances of the segmentation structure.

Input Segmentation Rectangle Sorting. As mentioned in Section 5, to provide the model with a structured format of the input segmentations we sort the rectangles by their origins (firstly by the

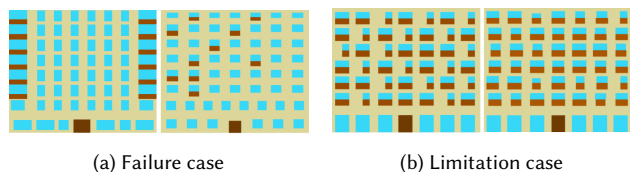


Fig. 8. The showcase of failure and limitation cases of our approach: (a) the model snowballs from one mistake and completely rearranges all balconies; (b) our grammar does not contain any productions which could recreate a balcony layout this irregular.

Y coordinate, then the X coordinate). We tested whether this preprocessing step provides actual benefits to the model’s ability to learn. We propose two more methods of ordering the input: (1) random order, (2) grouping the rectangles by their category and sorting the groups alphabetically. Figure 7c shows that while the alternative methods of structuring the input perform quite well on the training set, the model’s ability to generalize gets diminished, which is showcased by the poor validation loss in later epochs. We conclude that since a transformer is able to extract context information based on relative positions of tokens, encoding as much information in the ordering itself should benefit the learning process.

Dataset Size Dependence. The data that we use for training is procedurally generated by our data generation module. This allows us to generate as many facades as we require from the facade data distribution that the data generator represents. We use this fact to test how the amount of data the our model is trained on influences its ability to reconstruct facades. We generate 4 datasets of varying sizes—starting from 20k facades all the way up to 200k facades. Since the space of all possible facade segmentations is vast, we do not expect any data-point repeats, even in the largest dataset. Our experiments show that the dataset size has a big impact on the abilities of the model—the more data it was fed the better the results (cf. Figure 7a). We assume that this behavior is caused by the complexity of the function being learned which arises from subspaces, in the all possible segmentations space, that should evaluate to the same structure even though their sizings (and by consequence the sequence that represents them) differ vastly.

Learning Rate and Batch Size. We have performed multiple tests to identify what values of learning rate and batch size best fit our model. From the results (cf. Figures 7f and 7g) we conclude that learning rates equal to 0.0001 and 0.00001 both provide satisfactory results (we opt for the smaller value), while that batch size does not impact the result substantially as long as it’s not too big (we settled on a batch size of 32).

8 QUALITATIVE RESULTS

The qualitative results were generated on facades manually segmented into grids of rectangular boxes, and annotated. The segmentations have been crafted such that they match the terminals of our grammar and take around 5 minutes each to construct. For that task we have implemented a rudimentary segmentation interface. In practice, our goal would be to either use automatic segmentation

tools, based on machine learning methods [Selvaraju et al. 2021] or on interactive segmentation tools [Musialski et al. 2012]. However, generally, we consider that as given input which is not part of and essentially does not influence the contribution of this paper.

The results of the inference of the segmented inputs are depicted in Figure 9. Each facade is comprised of 5 images: (1) image of the facade being reconstructed, (2) the structural representation generated by the transformer model with default sizing parameters, (3) an optimized facade which sizing now matches the target facade, (4) and (5) variations of the target facade created by slightly modifying the procedural representation of it. The results show that our approach can successfully reproduce facades of different structures and styles while giving us the ability to generate brand new variations with little to no effort. Additionally, Figure 10 showcases renderings of the facades based on the resulting segmentations.

9 DISCUSSION AND LIMITATIONS

While our method reproduces a vast range of facades, it has limitations tied to the split-grammar language it relies on. If no derivation trees based on the grammar can reproduce a given facade, the model may not deliver a correct result (Figure 8). This can be mitigated by extending the grammar with more procedures and making them more general, which requires insight into architectural design. Additionally, the transformer model’s memory requirement scales proportionally to the sequence length squared, limiting facade sizes and detail levels.

A common failure case is the snowball effect during inference. If the model makes an error while generating the main structure, such as missing a segment on a floor, further generation can become scrambled (Figure 8). This can sometimes be rectified by manually fixing the error and running a partial inference from that point.

10 CONCLUSIONS AND FUTURE WORK

In this paper we proposed a transformer-based model for neuro-symbolic reconstruction of procedural shape representations. We proposed a semi-complex split grammar based on previous work on procedural architecture generation [Wonka et al. 2003].

As a main contribution we proposed an encoder-decoder model composed of two GPT-2 transformers. We trained our model on 200,000 procedurally generated pairs of facade segmentations and split grammar based procedures. The whole dataset was automatically generated using our proposed split-grammar based generator described in Section 4. In our current implementation, the presented method is able to closely recreate given input facades as procedures, including their sizing parameters.

The approach could be further developed by making the grammar more general, using just a couple of multi-purpose space partition productions. This would allow the model to potentially formulate more complex functions by itself, which would be an abstraction of those primitive splits. There is also room to optimize the sequence length that is passed to the model to enable representing larger and more detailed facades. Splitting the facade into smaller parts and generating their structural representations independently is a route worth exploring. Furthermore, a natural step for the method would be reconstructing 3D buildings as procedures.

REFERENCES

- Daniel G. Aliaga, Paul A Rosen, and Daniel R Bekins. 2007. Style grammars for interactive visualization of architecture. *IEEE Transactions on Visualization and Computer Graphics* 13, 4 (2007), 786–97. <https://doi.org/10.1109/TVCG.2007.1024>
- Rajeev Alur, Rastislav Bodik, Garvit Juniwal, Milo M. K. Martin, Mukund Raghothaman, Sanjit A. Seshia, Rishabh Singh, Armando Solar-Lezama, Emina Torlak, and Abhishek Udupa. 2013. Syntax-guided synthesis. *2013 Formal Methods in Computer-Aided Design* (2013), 1–8. <https://api.semanticscholar.org/CorpusID:6705760>
- Maximilian Bachl and Daniel C. Ferreira. 2019. City-GAN: Learning architectural styles using a custom Conditional GAN architecture. *ArXiv abs/1907.05280* (2019). <https://api.semanticscholar.org/CorpusID:195886591>
- John Warner Backus, Robert J. Beeber, Sheldon Best, Richard Goldberg, Lois M. Haibt, Harlan L. Herrick, Robert A. Nelson, David Sayre, Peter B. Sheridan, H. Stern, Irving Ziller, Robert A. Hughes, and Rgr Nutt. 1957. The FORTRAN automatic coding system. In *IRE-AIEE-ACM '57 (Western)*. <https://api.semanticscholar.org/CorpusID:13973980>
- Fan Bao, Michael Schwarz, and Peter Wonka. 2013. Procedural facade variations from a single layout. *ACM Transactions on Graphics (TOG)* 32 (2013), 1–13. <https://api.semanticscholar.org/CorpusID:18542228>
- Susanne Becker. 2009. Generation and application of rules for quality dependent facade reconstruction. *Isprs Journal of Photogrammetry and Remote Sensing* 64 (2009), 640–653. <https://api.semanticscholar.org/CorpusID:123628745>
- Daniel R. Bekins and Daniel G. Aliaga. 2005. Build-by-number: rearranging the real world to visualize novel architectural spaces. *VIS 05. IEEE Visualization, 2005.* (2005), 143–150. <https://api.semanticscholar.org/CorpusID:10252257>
- Martin Bokeloh, Michael Wand, and Hans-Peter Seidel. 2010. A connection between partial symmetry and inverse procedural modeling. *ACM Transactions on Graphics* 29, 4 (jul 2010), 104–114. <https://doi.org/10.1145/1778765.1778841>
- Moses Charikar, Eric Lehman, Ding Liu, Rina Panigrahy, Manoj Prabhakaran, Amit Sahai, and Abhi Shelat. 2005. The smallest grammar problem. *IEEE Transactions on Information Theory* 51 (2005), 2554–2576. <https://api.semanticscholar.org/CorpusID:6900082>
- Swarat Chaudhuri, Kevin Ellis, Oleksandr Polozov, Rishabh Singh, Armando Solar-Lezama, and Yisong Yue. 2021. Neurosymbolic Programming. *Found. Trends Program. Lang.* 7 (2021), 158–243. <https://api.semanticscholar.org/CorpusID:245107814>
- Ilke Demir and Daniel G. Aliaga. 2018. Guided Proceduralization: Optimizing Geometry Processing and Grammar Extraction for Architectural Models. *ArXiv abs/1807.02578* (2018). <https://api.semanticscholar.org/CorpusID:49659157>
- Tao Du, Jeevana Priya Inala, Yewen Pu, Andrew Spielberg, Adriana Schulz, Daniela Rus, Armando Solar-Lezama, and Wojciech Matusik. 2018. InverseCSG: automatic conversion of 3D models to CSG trees. *ACM Trans. Graph.* 37, 6, Article 213 (dec 2018), 16 pages. <https://doi.org/10.1145/3272127.3275006>
- Lubin Fan, Przemysław Musiański, Ligang Liu, and Peter Wonka. 2014. Structure completion for facade layouts. *ACM Transactions on Graphics (TOG)* 33 (2014), 1–11. <https://api.semanticscholar.org/CorpusID:15471241>
- Paul Guerrero, Milos Hasan, Kalyan Sunkavalli, Radomir Mech, Tamy Boubekour, and Niloy J. Mitra. 2022. MatFormer. *ACM Transactions on Graphics (TOG)* 41 (2022), 1–12. <https://api.semanticscholar.org/CorpusID:260484422>
- Brian Hempel, Justin Lubin, and Ravi Chugh. 2019. Sketch-n-Sketch: Output-Directed Programming for SVG. *Proceedings of the 32nd Annual ACM Symposium on User Interface Software and Technology* (2019). <https://api.semanticscholar.org/CorpusID:198895618>
- Martin Ilčík, Przemysław Musiański, Thomas Auzinger, and Michael Wimmer. 2015. Layer-Based Procedural Design of Façades. *Computer Graphics Forum (Proc. EURO-GRAPHICS 2015)* 34, 2 (may 2015), 205–216. <https://doi.org/10.1111/cgf.12553>
- R. Kenny Jones, Theresa Barton, Xianghao Xu, Kai Wang, Ellen Jiang, Paul Guerrero, Niloy J. Mitra, and Daniel Ritchie. 2020. ShapeAssembly: learning to generate programs for 3D shape structure synthesis. *ACM Trans. Graph.* 39, 6, Article 234 (nov 2020), 20 pages. <https://doi.org/10.1145/3414685.3417812>
- Tero Karras, Samuli Laine, and Timo Aila. 2018. A Style-Based Generator Architecture for Generative Adversarial Networks. *2019 IEEE/CVF Conference on Computer Vision and Pattern Recognition (CVPR)* (2018), 4396–4405. <https://api.semanticscholar.org/CorpusID:54482423>
- Diederik P. Kingma and Jimmy Ba. 2017. Adam: A Method for Stochastic Optimization. (2017). [arXiv:1412.6980](https://arxiv.org/abs/1412.6980) [cs.LG]
- Jae Joong Lee, Bosheng Li, and Bedrich Benes. 2024. Latent L-Systems: Transformer-Based Tree Generator. *ACM Trans. Graph.* 43, 1, Article 7 (Feb. 2024), 16 pages. <https://doi.org/10.1145/3627101>
- Kurt Leimer, Paul Guerrero, Tomer Weiss, and Przemysław Musiański. 2022. LayoutEnhancer: Generating Good Indoor Layouts from Imperfect Data. In *SIGGRAPH Asia 2022 Conference Papers (SA '22)*. Association for Computing Machinery, New York, NY, USA, Article 27, 8 pages. <https://doi.org/10.1145/3550469.3555425>
- Jun Li, Kai Xu, Siddhartha Chaudhuri, Ersin Yumer, Hao Zhang, and Leonidas Guibas. 2017. GRASS: generative recursive autoencoders for shape structures. *ACM Trans. Graph.* 36, 4, Article 52 (jul 2017), 14 pages. <https://doi.org/10.1145/3072959.3073637>
- Ziyang Li, Jiani Huang, and M. Naik. 2023. Scallop: A Language for Neurosymbolic Programming. *Proceedings of the ACM on Programming Languages* 7 (2023), 1463–1487. <https://api.semanticscholar.org/CorpusID:258060005>
- Markus Lipp, Peter Wonka, and Michael Wimmer. 2008. Interactive visual editing of grammars for procedural architecture. *ACM Transactions on Graphics* 27, 3 (aug 2008), 1. <https://doi.org/10.1145/1360612.1360701>
- Ilya Loshchilov and Frank Hutter. 2019. Decoupled Weight Decay Regularization. (2019). [arXiv:1711.05101](https://arxiv.org/abs/1711.05101) [cs.LG]
- Andelo Martinovic and Luc Van Gool. 2013. Bayesian Grammar Learning for Inverse Procedural Modeling. *2013 IEEE Conference on Computer Vision and Pattern Recognition* (2013), 201–208. <https://api.semanticscholar.org/CorpusID:419779>
- Markus Mathias, Andelo Martinovic, Julien Weissenberg, and Luc Van Gool. 2011. Procedural 3D Building Reconstruction Using Shape Grammars and Detectors. *2011 International Conference on 3D Imaging, Modeling, Processing, Visualization and Transmission* (2011), 304–311. <https://api.semanticscholar.org/CorpusID:8533912>
- Kaichun Mo, Paul Guerrero, Li Yi, Hao Su, Peter Wonka, Niloy J. Mitra, and Leonidas J. Guibas. 2019. StructureNet: hierarchical graph networks for 3D shape generation. *ACM Trans. Graph.* 38, 6, Article 242 (nov 2019), 19 pages. <https://doi.org/10.1145/3355089.3355627>
- Pascal Müller, Peter Wonka, Simon Haegler, Andreas Ulmer, and Luc van Gool. 2006. Procedural modeling of buildings. *ACM Transactions on Graphics* 25, 3 (jul 2006), 614. <https://doi.org/10.1145/1141911.1141931>
- Pascal Müller, Gang Zeng, Peter Wonka, and Luc van Gool. 2007. Image-based procedural modeling of facades. *ACM Transactions on Graphics* 26, 3 (jul 2007), 85–94. <https://doi.org/10.1145/1276377.1276484>
- Przemysław Musiański and Michael Wimmer. 2013. Inverse-Procedural Methods for Urban Models. In *Proc. of 1st Eurographics Workshop on Urban Data Modelling and Visualisation*, V. Besiuvesky and G. Tourre (Eds.). Eurographics Association, Girona, Spain, 31–32. <https://doi.org/10.2312/UDMV/UDMV13/031-032>
- Przemysław Musiański, Michael Wimmer, and Peter Wonka. 2012. Interactive Coherence-Based Façade Modeling. *Computer Graphics Forum* 31 (2012). <https://api.semanticscholar.org/CorpusID:10873890>
- Chandrakana Nandi, James R. Wilcox, Pavel Panchekha, Taylor Blau, Dan Grossman, and Zachary Tatlock. 2018. Functional programming for compiling and decompiling computer-aided design. *Proceedings of the ACM on Programming Languages* 2 (2018), 1–31. <https://api.semanticscholar.org/CorpusID:51729710>
- Chandrakana Nandi, Max Willsey, Adam Anderson, James R. Wilcox, Eva Darulova, Dan Grossman, and Zach Tatlock. 2019. Synthesizing structured CAD models with equality saturation and inverse transformations. *Proceedings of the 41st ACM SIGPLAN Conference on Programming Language Design and Implementation* (2019). <https://api.semanticscholar.org/CorpusID:263864332>
- Charlie Nash, Yaroslav Ganin, Ali Eslami, and Peter W. Battaglia. 2020. PolyGen: An Autoregressive Generative Model of 3D Meshes. *ArXiv abs/2002.10880* (2020). <https://api.semanticscholar.org/CorpusID:211296328>
- Wamiq Para, Paul Guerrero, Tom Kelly, Leonidas J Guibas, and Peter Wonka. 2021. Generative layout modeling using constraint graphs. In *Proceedings of the IEEE/CVF International Conference on Computer Vision*. 6690–6700.
- Despoina Paschalidou, Amlan Kar, Maria Shugrina, Karsten Kreis, Andreas Geiger, and Sanja Fidler. 2021. ATISS: Autoregressive Transformers for Indoor Scene Synthesis. In *Advances in Neural Information Processing Systems (NeurIPS)*.
- Przemysław Prusinkiewicz and Aristid Lindenmayer. 1990. *The algorithmic beauty of plants*. Springer-Verlag New York, Inc., New York, 228 pages. <http://portal.acm.org/citation.cfm?id=83596>
- Alec Radford, Jeffrey Wu, Rewon Child, David Luan, Dario Amodei, Ilya Sutskever, et al. 2019. Language models are unsupervised multitask learners. *OpenAI blog* 1, 8 (2019), 9.
- Elad Richardson, Yuval Alaluf, Or Patashnik, Yotam Nitzan, Yaniv Azar, Stav Shapiro, and Daniel Cohen-Or. 2020. Encoding in Style: a StyleGAN Encoder for Image-to-Image Translation. *2021 IEEE/CVF Conference on Computer Vision and Pattern Recognition (CVPR)* (2020), 2287–2296. <https://api.semanticscholar.org/CorpusID:220936362>
- Hayko Riemenschneider, Ulrich Krispel, Wolfgang Thaller, Michael Donoser, Sven Havemann, Dieter W. Fellner, and Horst Bischof. 2012. Irregular lattices for complex shape grammar facade parsing. *2012 IEEE Conference on Computer Vision and Pattern Recognition* (2012), 1640–1647. <https://api.semanticscholar.org/CorpusID:6985760>
- Nora Ripperda and Claus Brenner. 2009. Application of a Formal Grammar to Façade Reconstruction in Semiautomatic and Automatic Environments. <https://api.semanticscholar.org/CorpusID:2240170>
- Daniel Ritchie, Paul Guerrero, R. Kenny Jones, Niloy J. Mitra, Adriana Schulz, Karl D. D. Willis, and Jiajun Wu. 2023. Neurosymbolic Models for Computer Graphics. *Computer Graphics Forum* 42, 2 (2023), 545–568. <https://doi.org/10.1111/cgf.14775> <https://onlinelibrary.wiley.com/doi/pdf/10.1111/cgf.14775>
- Pratheba Selvaraju, Mohamed Nabail, Marios Loizou, Maria I. Maslioukova, Melinos Averkiou, Andreas C. Andreou, Siddhartha Chaudhuri, and Evangelos Kalogerakis. 2021. BuildingNet: Learning to Label 3D Buildings. *2021 IEEE/CVF International Conference on Computer Vision (ICCV)* (2021), 10377–10387. <https://api.semanticscholar.org/CorpusID:2240170>

- [//api.semanticscholar.org/CorpusID:238211970](https://api.semanticscholar.org/CorpusID:238211970)
- Armando Solar-Lezama, Liviu Tancau, Rastislav Bodik, Sanjit A. Seshia, and Vijay A. Saraswat. 2006. Combinatorial sketching for finite programs. In *ASPLOS XII*. <https://api.semanticscholar.org/CorpusID:15367706>
- O. St'ava, Bedrich Beneš, R. Mech, Daniel G. Aliaga, and P. Krištof. 2010. Inverse Procedural Modeling by Automatic Generation of L-systems. *Computer Graphics Forum* 29, 2 (2010), 665–674. [http://www.cs.jhu.edu/\\$\sim\\$smisha/ReadingSeminar/Papers/Stava10.pdf](http://www.cs.jhu.edu/\simsmisha/ReadingSeminar/Papers/Stava10.pdf)
- George Nicholas Stiny. 1975. Pictorial and formal aspects of shape and shape grammars and aesthetic systems. (1975), 417. <http://portal.acm.org/citation.cfm?id=907151>
- Cheng Sun, Yiran Zhou, and Yunsong Han. 2022. Automatic generation of architecture facade for historical urban renovation using generative adversarial network. *Building and Environment* (2022). <https://api.semanticscholar.org/CorpusID:245949658>
- Jerry O. Talton, Lingfeng Yang, Ranjitha Kumar, Maxine Lim, Noah D. Goodman, and Radomir Mech. 2012. Learning design patterns with bayesian grammar induction. *Proceedings of the 25th annual ACM symposium on User interface software and technology* (2012). <https://api.semanticscholar.org/CorpusID:17007327>
- Olivier Teboul, Iasonas Kokkinos, Loïc Simon, Panagiotis Koutsourakis, and Nikos Paragios. 2011. Shape grammar parsing via Reinforcement Learning. *CVPR 2011* (2011), 2273–2280. <https://api.semanticscholar.org/CorpusID:1393392>
- Olivier Teboul, Iasonas Kokkinos, Loïc Simon, Panagiotis Koutsourakis, and Nikos Paragios. 2013. Parsing Facades with Shape Grammars and Reinforcement Learning. *IEEE Transactions on Pattern Analysis and Machine Intelligence* 35 (2013), 1744–1756. <https://api.semanticscholar.org/CorpusID:6700628>
- Alexander Toshev, Philippos Mordohai, and Ben Taskar. 2010. Detecting and parsing architecture at city scale from range data. *2010 IEEE Computer Society Conference on Computer Vision and Pattern Recognition* (2010), 398–405. <https://api.semanticscholar.org/CorpusID:432133>
- Radim Tyleček and Radim Šára. 2013. Spatial Pattern Templates for Recognition of Objects with Regular Structure. In *Proc. GCPR*. Saarbrücken, Germany.
- Carlos A. Vanegas, Daniel G. Aliaga, Peter Wonka, Pascal Müller, Paul A. Waddell, and Benjamin Watson. 2010. Modelling the Appearance and Behaviour of Urban Spaces. *Computer Graphics Forum* 29, 1 (mar 2010), 25–42. <https://doi.org/10.1111/j.1467-8659.2009.01535.x>
- Ashish Vaswani, Noam Shazeer, Niki Parmar, Jakob Uszkoreit, Llion Jones, Aidan N Gomez, Łukasz Kaiser, and Illia Polosukhin. 2017. Attention is all you need. In *Advances in neural information processing systems*, 5998–6008.
- Xinpeng Wang, Chandan Yeshwanth, and Matthias Nießner. 2020. SceneFormer: Indoor Scene Generation with Transformers. *arXiv preprint arXiv:2012.09793* (2020).
- Julien Weissenberg, Hayko Riemenschneider, Mukta Prasad, and Luc Van Gool. 2013. Is There a Procedural Logic to Architecture? *2013 IEEE Conference on Computer Vision and Pattern Recognition* (2013), 185–192. <https://api.semanticscholar.org/CorpusID:6936441>
- Emily Whiting, John Ochsendorf, and Frédo Durand. 2009. Procedural modeling of structurally-sound masonry buildings. In *ACM SIGGRAPH Asia 2009 papers on - SIGGRAPH Asia '09*, Vol. 28. ACM Press, New York, New York, USA, 1. <https://doi.org/10.1145/1661412.1618458>
- Thomas Wolf, Lysandre Debut, Victor Sanh, Julien Chaumond, Clement Delangue, Anthony Moi, Pierric Cistac, Tim Rault, Rémi Louf, Morgan Funtowicz, Joe Davison, Sam Shleifer, Patrick von Platen, Clara Ma, Yacine Jernite, Julien Plu, Canwen Xu, Teven Le Scao, Sylvain Gugger, Mariama Drame, Quentin Lhoest, and Alexander M. Rush. 2020. Transformers: State-of-the-Art Natural Language Processing. In *Proceedings of the 2020 Conference on Empirical Methods in Natural Language Processing: System Demonstrations*. Association for Computational Linguistics, Online, 38–45. <https://www.aclweb.org/anthology/2020.emnlp-demos.6>
- Peter Wonka, Michael Wimmer, François Sillion, and William Ribarsky. 2003. Instant architecture. *ACM Transactions on Graphics* 22, 3 (jul 2003), 669. <https://doi.org/10.1145/882262.882324>
- Fuzhang Wu, Dong-Ming Yan, Weiming Dong, Xiaopeng Zhang, and Peter Wonka. 2013. Inverse procedural modeling of facade layouts. *ACM Transactions on Graphics (TOG)* 33 (2013), 1 – 10. <https://api.semanticscholar.org/CorpusID:13525826>
- Fuzhang Wu, Dong-Ming Yan, Weiming Dong, Xiaopeng Zhang, and Peter Wonka. 2014. Inverse procedural modeling of facade layouts. *ACM Trans. Graph.* 33, 4, Article 121 (jul 2014), 10 pages. <https://doi.org/10.1145/2601097.2601162>
- Rundi Wu, Chang Xiao, and Changxi Zheng. 2021. DeepCAD: A Deep Generative Network for Computer-Aided Design Models. *2021 IEEE/CVF International Conference on Computer Vision (ICCV)* (2021), 6752–6762. <https://api.semanticscholar.org/CorpusID:234789948>
- Hao Zhang, Kai Xu, Wei Jiang, Jinjie Lin, Daniel Cohen-Or, and Baoquan Chen. 2013. Layered analysis of irregular facades via symmetry maximization. *ACM Transactions on Graphics (TOG)* 32 (2013), 1 – 13. <https://api.semanticscholar.org/CorpusID:10500417>

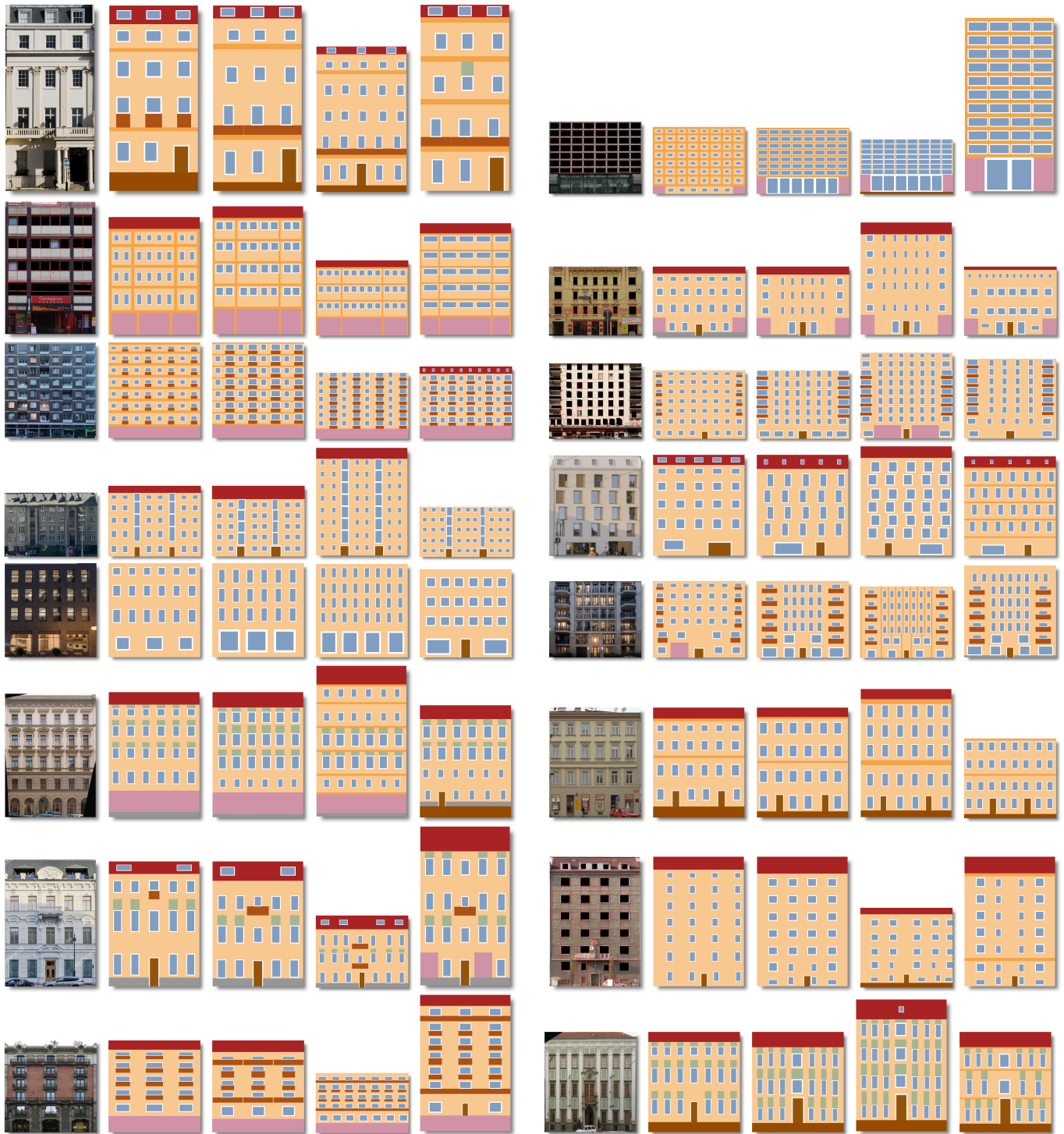


Fig. 9. Results of our method: Each sequence of 5 images first depicts the original input image (partially from [Musialski et al. 2012]). The second image shows the structural reconstruction delivered by the transformer model, the third image shows the result after sizing optimization, and the last two results are procedurally generated variations. Best seen in close-up in the electronic version.



Fig. 10. Rendering of the results of our method including material properties assigned to different segmentation classes. Each sequence shows the input image, the procedural reconstruction, and two variations of the same facade procedure. Best seen in close-up in the electronic version.